Grain Boundary Relaxation in Doped Nano-grained Aluminum

[1]Wenye Ye, [1]Jake Hohl, [1]Mano Misra, [2]Yiliang Liao, [1]Leslie T Mushongera*

[1]Department of Chemical & Materials Engineering, University of Nevada, Reno, Reno, NV, USA

[2]Department of Industrial and Manufacturing Systems Engineering, Iowa State University, Ames, IA 50011, USA

*Corresponding author: lmushongera@unr.edu**

Abstract

Simulation studies are done to understand the role of dopants that segregate preferentially to grain boundaries on the stability of nanocrystalline aluminum. A dopant design framework based on thermodynamic principles, is used to identify the specific dopant type with the highest potential to segregate to grain boundaries in nanocrystalline aluminum. Various elements are evaluated as potential dopants and magnesium is identified to have the highest tendency to segregate to grain boundaries and release the excess free energy leading to the relaxation of the grain boundaries. A systematic combination of atomic structure analysis is then done to correlate grain boundary relaxation and the mechanical response of the magnesium-doped nanocrystalline aluminum at ambient temperature. The atomistic simulations reveal that the preferential partitioning of magnesium dopants to the grain boundaries reduces the excess volume within this region which stabilizes the nanostructure. At low contents, the magnesium dopants are observed initially partition to the grain boundaries, but once saturation of the grain boundaries is reached, excess dopants are accommodated in the crystalline interiors. It is found that the addition of the magnesium dopants even in the dilute limit, enhances the strength of the nanocrystalline aluminum. The formation of large, disordered GBs in doped nanocrystalline aluminum under tensile load allowed it to accommodate the deformation and prohibit crack growth.

Keywords: Nanocrystalline Aluminum; Grain Boundary Relaxation; Modeling

1. Introduction

Nanocrystalline metals which consist of grain sizes of typically less than 100 nanometers have been attracting increasing interests due their unique properties. In having the small grain

sizes, nanocrystalline have an enormous amount of interfacial material, largely in the grain boundary region [1]. Nanocrystalline metals exhibit properties that are different and often superior in comparison to the conventional coarse-grained materials. For example, nanocrystalline metals have enhanced mechanical properties including ultrahigh strength and high hardness [2-5]. As a good measure - the hardness and tensile strength of nanocrystalline aluminum is seven [5] and up to ten folds [6,7], respectively, higher than of conventional polycrystalline counterparts. Furthermore, nanocrystalline metals recover significant amount of plastic deformation, which in convectional polycrystalline materials is usually considered permanent, after unloading [18,30]. These qualities derive from the large fraction of interfacial materials that reside at grain boundaries.

Maintaining the nanocrystalline grain structure has however limited the application of nanocrystalline metals in critical structural components [8-10]. Nanocrystalline metals lack long-term stability, rendering them unsuitable for critical structural applications [See Ref. [11] for comprehensive review]. The compromised stability of nanocrystalline metals is attributed to high-energy grain boundaries associated with the small grain size. Grain boundaries are degenerate in nature as compared to the crystalline interior; thus, they are associated with excess free energies. As a result, nanocrystalline metals are susceptible to kinetic phenomena that lead to changes of the nanostructures. To reduce the excess free energy, the nanocrystalline grains coarsen, that is, large grains grow at the expense of smaller ones. This coarsening phenomenon is directly related to the grain boundary state (structure and energy). Coarsening causes the nanocrystalline metals to lose their extraordinary mechanical properties [5,7]. Atomic rearrangements, in which atoms under the influence of the local atomic environment, overcome energy barriers to move, characterizes the dynamics of grain boundaries in nanocrystalline materials that are ultimately responsible for the degradation of the mechanical properties. Therefore, to maintain the desirable mechanical properties of nanocrystalline metals, it is necessary to preserve the structure of nanocrystalline metals at the atomic scale.

Since pure nanocrystalline metals consists of two physically and chemically distinct regions namely, the bulk grain and grain boundaries, the preferential enrichment of dopants at the grain boundaries has been used to tailor these materials. Doping the grain boundaries in nanocrystalline metals with a stable dopant provides the opportunity to reduce kinetic phenomena like coarsening, thus increase the stability of nanocrystalline metals [12-16]. A

baseline of dopants that segregate preferentially to the grain boundaries in nanocrystalline metals was built in Ref. [19]. In support, various thermodynamic studies have showed the positive segregation enthalpy of mixing between solvent-solute (dopant) pair, drives solute (dopant) segregation at high-energy defect sites such as grain boundaries [20-24]. Additionally, the thermodynamic theories have shown that the interaction of solutes (dopants) with the high energy grain boundaries can significantly reduce the Gibbs free energy of mixing, in the non-crystalline grain boundaries which leads to a reduction in the global energy of the system. The reduction indicates a relaxation of non-stable grain boundaries to stable configurations. Annealing experiments have shown increasing order within the non-lattice sites in doped nanocrystalline [25]. The segregation of atoms could serve as a simple yet effective alleviation mechanism to reduce the number of defects in the grain boundary region that could otherwise reduce the stability of the nanostructure.

In powder-based manufacturing of nanocrystalline metals, energy typically stores in the form of excessive grain boundaries, which lowers the activation energy for the nucleation of dislocations [5,7]. As a result, grain boundaries act as the easy dislocation nucleation sites. Under applied loads, these high energy grain boundaries can glide to the equilibrium configuration to release excess energy. The reduction in grain boundary energy can lead to an increase in resistance to grain boundary gliding and increase the difficulty in dislocation nucleation and motion [6,17]. Both increase the strength of nanocrystalline materials. However, the achievable strength in nanocrystalline metals by the stress-induced grain boundary relaxation significantly is limited by the risk of grain growth. The excess stored energy in in grain boundary relaxation provides the driving force for grain growth, thus compromise the stability of nanocrystalline metals [11,17-19]. It is essential to reduce the grain boundary energy and increase the stability of nanocrystalline metals. Despite the vast body of work on nanocrystalline metals, the precise GB mechanisms governing the stability and mechanical response of these systems are yet to be fully established and remain the subject of conjecture.

The objective of this work is to understand the influence of preferentially segregating dopants on grain boundary relaxation, and the subsequent effect on plastic deformation mechanisms in nanocrystalline aluminum (NC Al). Based on thermodynamic principles, a highly efficient dopant design framework [32] is used to identify the specific dopant type that interacts with high energy grain boundaries in NC Al to release the excess free energy in the boundaries. Emphasis

is put on improving the stability of the NC Al against grain growth and phase separation. A combined molecular dynamic (MD) and Monte Carlo (MC) method is then used to analyze grain boundary stability in NC Al with emphasis on dopant distribution and its effect on the mechanical response. The atomic structures used in this work were generated in a manner that allowed the systematic variation of the structure (chemistry) of the grain boundaries but keeping the grain size constant. Thus, the influence of grain size on strength was constant in all the atomistic simulations.

In the following section, the influence of dopants on the stability of the NC Al against grain growth and phase separation is assessed. Section 3 presents results on the thermodynamically stable nanocrystalline states in NC Al-Mg, followed by the analysis of the role of the Mg dopants on the mechanical response before concluding in Section 4.

2. Assessment of nanocrystalline stability

Thermodynamic modeling was done to evaluate the efficacy of various dopant types in stabilizing the nanocrystalline structure of Al. For this purpose, a standard regular solution model for binary nanocrystalline alloys presented in prior work [32], was employed to assess the stability of nanocrystalline Al-dopant alloyed pairs against both phase precipitation and grain enlargement.

2.1. Stability against grain enlargement

Fifty-one potential dopant elements were assessed utilizing the thermodynamic framework for their ability segregate to the grain boundaries and stabilize the nanocrystallline aluminum structure. For each element, a 3D stability surface was created to show a variation in the material's Gibbs free energy as a function of grain size and grain boundary solute content.

The minimum in each material's surface denotes the respective grain size and grain boundary solute content at which stability of the microstructure is achieved for a given global dopant content. Fig. 1 shows 3D free energy surfaces which describe how the nanostructures energy changes as a function of its grain boundary dopant content (X_{gb}), which is an approximation for the system's degree of segregation, and as a function of the final nanostructure's average grain size (d). A minimum in this surface at a nanocrystalline grain size denotes a state of stability at which the benefit to material properties of a nanocrystalline structure are retained. From this data, the stable nanocrystalline grain size and the degree of dopant segregation to the grain boundaries of the material was established. A convex shape indicated that the dopant addition

resulted in NC stability while a dopnat that led to a concave shape resulted in an unstable NC state. From this analysis, it was found that Mg – by virtue of having a free energy curve with a convex shape, exhibited the necessary characteristics to segregate to the grain boundary in NC-Al and promote a state of stability in the nanocrystalline regime.

2.2. Stability against phase separation

Additionally, secondary phase precipitation was assessed through the use of an empirical stability criterion derived from the results of the thermodynamic model and shown in Fig. 2. This stability criterion, $\Delta H_{seg}/(\Delta H_{mix})^a = c$ was used as a rapid screening tool for dopant element's efficacy in stabilizing the aluminum nanostructure by comparing the enthalpies of mixing and segregation for each material system as by the stability map's axes. The criterion was calibrated using regression analysis of the original regular nanocrystalline regular solution model's stability predictions utilizing a large dataset of binary nanocrystalline alloys which yielded the fit coefficients $a = 0.567$ and $c = 4.425$. From this criterion it was observed that stability against phase precipitation was predicted for only Al-Mg, with a high positive enthalpy of segregation and a low positive enthalpy of mixing, under a content limit determined by the onset of phase precipitation above 13% Mg. This result can be seen by noting that the alloy is the only one which lies above the metastable curve of the stability map. In this map, the alloys lying above the metastable line are confidently stable against both grain growth and phase precipitation up to their melting point. Those alloys lying between the metastable and unstable curves are those for which stability may or may not be present at varying temperatures, and rapid onset of phase precipitation under changes in temperature are possible. Those alloys lying under the unstable line reliably precipitate secondary phases and are considered to be unstable as they undergo rapid changes in material properties due to these effects. Being that additional global dopant content up to the 13% limit serves to increase the microstructure's stability, as assessed by the analysis of the system's Gibbs free energy surfaces, higher dopant contents under this limit are preferential. Additionally, within this content range, additions of the dopant element serve to reduce the average grain size of the produced nanostructure, and increase the degree of dopant segregation to the grain boundary of the material. For example, the equilibrium grain size was 8 nm when 3% Mg was added to NC Al and 9.9 nm when 10% Mg added.

3. Atomistic mechanisms influencing stability of NC Al

Three-dimensional (3D) equiaxed NC-Al structures were generated with an average grain size of 8 nm predicted from the thermodynamic modeling. The nanostructures were carefully generated to replicate experimental nanocrystalline metals capable of realistically capturing their evolution while providing computational efficiency. The 3D atomic structures of dimension $(200Å)^3$, with 10 equiaxed grains were generated based on a random (Poisson point process) Voronoi tessellation using the Atomsk software [29]. Each of the generated 3D nanocrystalline atomic structures contained 483,084 aluminum atoms and had grain sizes in the range of 8~12nm by assuming the grains are spherical. Periodic boundary conditions were applied along *x*, *y* and *z* directions, which created an infinitely large system such that those atoms placed outside of simulation box could be wrapped back inside. Samples prepared in this way were then relaxed in using MD in LAMMPS for 1ns at 300K and constant pressure.

3.1. Thermodynamically-preferred nanocrystalline states

Based on predictions from section 2, Mg, was chosen as the dopant element. Recent studies have found that the volume fraction of grain boundaries can be in excess of 10-25% for a nanostructured metal with an average grain size of 10nm [31]. Therefore, given the degenerate nature of the grain boundaries, a majority of the dopants were expected to segregate to the grain boundaries. Mg atoms were added randomly to a pure NC Al nanostructure, to produce compositions of NC Al-3, -5, -7 and -10 at. % Mg. The maximum dopant content was chosen based on preliminary thermodynamic calculations using energy minimization principles which showed that beyond 10 at. % Mg, second phase precipitates form in NC Al [32]. The precipitation of the second phase precipitates due to excess dopant can disrupt the necessary segregation required for grain stability.

The embedded-atom method (EAM) developed by Ref. [33] which describes the pairwise interactions for Al-Mg structures in a generalized form was used in the simulations. A hybrid method involving Monte Carlo (MC) and molecular dynamic (MD) was used to add the Mg dopants to the pure NC-Al and then relax the structures to create a low energy state. The MC/MD simulations were done at 300 K. This approach performed iterative transmutational MC steps, which sampled the canonical ensemble followed by MD simulations. The MC run involved randomly selecting either a solvent or dopant atom and swapping it with the other species. The trial moves were accepted or rejected based on the Metropolis algorithm. This algorithm calculated the acceptance probability based on energetic change during atomic swaps.

The low-energy state was necessary so that the atomic structures reproduced the quantum mechanical values for relative energy and geometries in a more accurate way.

To predict the thermodynamically preferred nanocrystalline states, the 3D nanocrystalline structures were simulated for 4 ns at temperatures of 300 K. Considering the computational resources, the time of simulation in this study is adequate to provide thermodynamic information about the dopant's role on the stability of the nanocrystalline structures. Under the condition of canonical ensemble (i.e., NVT conditions), where three parameters of the thermodynamic system were fixed throughout the simulation: the absolute temperature (T), the number of atoms (N), and the volume (V). The system searched for conformational state without changing the grain morphologies in the nanocrystalline structure. In order to get a detailed picture of the atomic dynamics within grain boundaries various cross-sectional views of the nanocrystalline structures were analyzed. The Ovito package [34] was used the analysis of chemical and defect distributions using the common neighbor analysis (CNA) method [35]. The method indexes each atom in the nanocrystalline structure according to its local atomic coordination. Two-dimensional (2D) sections of NC Al-3, -5, -7 and -10 at. % Mg are shown in Fig. 3 at 0 ns and 4 ns. Al (bulk) atoms are colored in green; Al (grain boundary) atoms are colored in white and Mg dopant atoms are colored in red. At 0 ns (top row), the atomic structure was characterized by an almost uniform distribution of Mg atoms within the nanostructure. The non-crystalline boundaries are characterized by atomic disorder thus are high-energy regions relative to the crystallite interior(s) and are therefore susceptible to both structural and chemical modifications. This modification of the grain boundaries in the chemical sense is apparent after 4 ns (bottom row). The nanocrystalline structures evolved to contain high Mg dopants in the grain boundaries relative to the interior of the grains. The partitioning of Mg dopants to the grain boundaries continued with time leading to a transition to thermodynamically stable nanocrystalline structures. The atomistic simulations revealed that the segregating Mg atoms occupy the free volume within the grain boundaries which effectively reduces the energy within this region.

3.2. Influence of Mg dopants on the local grain boundary state

Because the sample with 3 at. %, 5 at. % and 7 at. % Mg had a relatively low global dopant content, the segregation to the grain boundaries was clearly noticeable. Although the change was not that obvious in samples with 7 at. % Mg, the general trend was that Mg atoms preferentially partitioned to the grain boundaries. This segregation behavior can be clearly seen in region of

interest (ROI) in the grain boundary region marked by the dashed square in Fig 4. It is apparent that dopant atoms (red) segregate to the grain boundary at the end of simulation, compared with the number of dopant atoms at the beginning, the dopant atoms at grain boundary obviously increased. It was found that at low contents, most magnesium dopants initially partition to the grain boundaries, but once saturation of the grain boundaries is reached, excess dopants were then accommodated in the crystalline interiors. To get a quantitative picture of the segregation behavior, the Mg concentration in the boundaries is calculated as $C_{Mg}^{GB} = N_{Mg}^{GB}/A^{GB}$ where N_{Mg}^{GB} is the number of Mg dopant atoms in the boundaries, and A is the total grain boundary volume in the nanostructure. The Voronoi tessellation method was used to calculate the grain boundary area. In Fig. 4, the Mg content in the grain boundaries of all simulated structures gradually reached a saturation state after a few nanoseconds in the simulations. The time for each nanostructure to reach its saturation state varied. The saturated time for NC Al-3, -5, -7 and -10 at. % Mg was reached at 3.8, 3.6, 3.2 and 3.1ns, respectively. A large global dopant content leads to a large concentration of residual dopants in the bulk. A large content of residual dopants in the bulk grain provides a driving force for the precipitation of secondary phases which could lead to embrittlement [36].

The transformation of the nanocrystalline structure is driven by the minimization for the grain boundary energy which led to the relaxation of the grain boundaries. To get estimates of the grain boundary energy as affected by the segregation of the Mg dopants, the following formulas are used. First, the energy the grain boundary ensemble in the Al nanostructure without dopants was estimated as

$$E_{0,GB} = \sum_{i \in V} \frac{E_i^{GB} - E_i^{bulk}}{A} \qquad (1)$$

was used, where E_i^{GB} is the energy of Al atoms at a selected grain boundary with an area of A, E_i^{bulk} is the bulk energy of Al atoms in reference bulk grain relatively far away from the selected grain boundary. V is the volume of the whole nanostructure. The energy of the grain boundary ensemble of the Al nanostructure without dopants was estimated as

$$E_{GB} = E_{0,GB} - \chi \frac{E_{seg}}{A} \qquad (2)$$

where E_{seg} is the segregation energy per Mg dopant atom, χ is the total number of Mg dopants within the grain boundary of area A. The segregation energy describes the energy difference

between the bulk and GB with dopants, it is equivalent to the enthalpy ΔH^{seg} in the dilute limit of dopants in the nanostructure [37]. We acknowledge that calculating the realistic grain boundary in atomistic modeling due to the disorder of grain boundary structures and their interconnected nature. Although estimates of the grain boundary energies using Eq. (1) and (2) deviated from the absolute values, we nonetheless believe that we got an idea in the relative sense, of the how the grain boundary energies vary in the nanostructures. To get an idea of how the energy, two calculations of the energy of the grain boundaries ensemble were done using Eqs (1) and (2) at the at the beginning and end of the simulation. The addition of Mg to pure nanocrystalline aluminum led to a reduction in the grain boundary energy. It was observed that as the amount of Mg atoms added into the nanocrystals increases, the grain boundary energy decreases. The atomistic simulations revealed that the segregating Mg atoms occupy the free volume within the boundaries which reduces the grain boundary energy. Similar findings have been observed in Ref. [38], it was observed that a larger substitutional dopant can efficiently reduce the excess free volume and thus leading to a reduction the grain boundary energy. The reduction in grain boundary energy provides evidence of the relaxation of the grain boundaries.

3.3. Influence of Mg dopants on mechanical behavior of NC structures

Considering the thermodynamically preferred NC states obtained from section III with dopants at grain boundaries as initial input, strain-controlled virtual tensile and compressive tests were performed to understand the implications of grain boundary segregation on the mechanical response and deformation pathways. A uniaxial load was given from both sides of the atomic structure along the *x*-direction with a strain rate of 10^{10} s^{-1}. The Nose-Hoover (NH) barostat was used in *x*-, *y*-, and *z*-directions to keep the temperature at 300 K during the course of the mechanical tests. To account for the Poisson effect, the NH barostat also allowed to maintain a constant pressure in *x*- and *y*-directions such that the 3D structures were free to change in these directions.

The simulated stress-strain curves for the different crystalline structures with different dopant contents are shown in Fig. 5a and b. The plots show that for both tensile and compressive loading conditions, nanostructures containing Mg dopants have better strength than NC Al. Similar findings have been observed in experiment [26], where it was shown that alloying Al with Mg leads to better mechanical properties than of the pure Al. It is intuitive to say these mechanical properties will improve as the global Mg dopant content is increased. Similar

findings have been observed in experiment [39-41], where it was shown that alloying Al with Mg leads to better mechanical properties than of the pure Al. However, this apparently is not always the case as can be seen in Figs. 5. In Fig. 5c, under the tensile loading condition, a dopant content of 3% and 5% results in more or less the same yield strength. However, as the dopant content is increased from 5% to 10%, the yield strength of Al-Mg decreases. This indicates that the nanostructures generally have higher tensile yield strengths when the global Mg dopant content is in the dilute limit. However, under the compressive test, (Fig. 5d), an opposite trend in the yield strength is observed. The yield strength increased with the increasing Mg contents.

3.3.1 Grain boundary thickening and its effect on deformation

Two peculiar trends are observed in the stress-strain curves under both tensile and compressive loading. The stress-strain curve is characterized by a sudden drop in the flow stress in the structures. This trend is consistent with observations in experiment for nanocrystalline materials during tensile testing [42]. Another unique trend of simulated stress-strain curves is in the form of serrated flow curves at large strains. This trend in the flow curves was observed in the experimental stress-strain curves for NC Al-Mg [43]. To understand the atomistic mechanisms governing the observed stress-strain response, the evolution of the nanocrystalline structures was analyzed. The deformation mechanisms of the grain boundaries are very complicated due to that they can be affected by many factors. The atomistic studies revealed that the driving force for the initial deformation of the grain boundaries is the shear stress difference. Figure 7(c)-(e) shows the evolution of the atomistic structure for NC Al and (f)-(h) for NC Al-Mg under a tensile load. Under the tensile load, damage of the nanostructure involves two phenomena: grain evolution and intergranular cracking - with the latter leading to failure. As can be seen in Fig. 6, the evolution of the nanostructures occurred through migration and dissociation of some grain boundaries. This phenomenon occurred much faster in pure NC-Al than in NC Al-Mg to accommodate the tensile deformation. At the same time, cracks nucleated at various sites along the GBs. The formation of the cracks occurred much earlier in the pure NC Al. For example, the crack forming between grains #2 and #5 appeared at a strain of $\varepsilon = 0.09$ while it nucleated at $= 0.115$ in NC Al-Mg. A closer look at a region of interest (ROI) in NC Al (Fig. 6c) reveals that crack formation started in regions of GBs with large voids. Looking at Figs. 6 and 7, it is clear that the segregation of the Mg dopants stabilized the GBs. Under a given strain, the

cracks were reduced in size as the global Mg content was increased. Such a trend in the reduction of crack size was observed throughout the whole volume of the nanostructures.

The stress-driven migration of the grain boundaries considerably contributed to plastic flow in the nanocrystalline structures. The nanocrystalline structures exhibit various configurations of grain boundaries ranging from quasi-planar to curved. The deformation mechanisms of the quasi-planar grain boundaries were generally different from those of the curved grain boundaries. In early-stage deformation of the curved grain boundaries, the migration of the grain boundaries occurred via a shuffling motion whereby atoms moved form from the bulk crystal to the grain boundaries along the (111) surface. The deformation of the curved grain boundaries at low strain was observed to be easier than that of the quasi-planar ones due to the opposing forces due to the movement between two neighboring grains with curved grain boundaries. Furthermore, As the dopant content was increased, large, disordered GBs and triple junctions which contained a relatively large fraction of atoms was observed. The formation of large GBs essentially allowed them to better accommodate the deformation and prohibit crack growth. The thickening of the GBs was observed to occur in all Al-Mg structures under a tensile load, however, this phenomenon did not occur in pure Al.

3.3.2 Analysis of grain boundary-mediated deformation

As the structures evolved under both loading conditions, a slip to grain boundary-mediated deformation transition was observed. The onset of plastic deformation corresponded to the moment when the first partial dislocation was emmitted from the grain boundaries. In the initial stages of plasticity, slip was characterized by partial dislocations that crossed some of the grains leaving behind multiple stacking faults. The partial dislocations and stacking faults were observed in both NC Al and NC Al-Mg structures. The disordered grain boundaries were the sources and sinks for the partial dislocations during the plastic deformation processes. The partial dislocations nucleated at the grain boundaries before propagating into the bulk. The 2D sections in Fig. 6 and Fig. 7 show the development of extended partials in some grains under tensile condition. The emission of the partials was triggered by unusual atomic shuffling and migration of the grain boundaries. The interaction of the partial dislocations and other features in the nanocrystal triggered the serrations in the flow curves in Fig. 5. The serrations where generated due to the dynamic competition between the diffusing atoms and propagating partial dislocations. This effect curve occurred when the atomic motion was considerably faster than the

motion of partial dislocations through the bulk grain. As a result, the motion of the partial dislocations was blocked by the atoms. These blocked partial dislocations were then only released with further deformation, which resulted in a decrease in the flow stress. Grain boundary relaxation was observed was observed during the absorption of the core of the partial. This repeated dislocation block and release mechanism by the atoms resulted in serrations in the flow curve. No trailing partial was observed due to relaxation of the grain boundary that occurred during and after the nucleation and absorption of the partial. This is due to that the relaxation of the grain boundaries reduced the local stress to the levels that do not favor the emission of the trailing partial.

Deformation twins were observed in the nanocrystalline structures under both loading conditions. This typically occurred at high strain with the formed deformation twins being coherent along the (111) twinning planes. The simulations revealed different mechanisms by which the deformations twins formed. In some instances, the deformation twins formed from partials released from the grain boundary sources. During plastic deformation, many stacking faults were transformed into twins at high strain due to interaction between multiple stacking faults and grain boundaries. As a result of this interaction, the stacking faults expanded which increased their energy making the transition to twins energetically favorable. The presence of deformation twins can be considered to be unique because no deformation twinning has been observed in coarse-grained Al. Recently, transmission electron microscopy examinations [38] have shown that at large plastic deformation, twinning can occur in nanocrystalline metals. Twins were not observed in pure Al nanostructures under tension. The deformation twins were observed in NC Al-3, -5, -7 and -10 at. % Mg formed at relatively higher strain. A high stress or high strain is needed to activate the deformation twinning mechanisms, making them more prevalent in nanocrystalline metals than in their coarse-grained counterparts. Under a compressive load (Fig. 8), some deformation twins formed via breakdown of the grain boundaries and migration of the segments leaving behind two coherent twin boundaries. The newly formed deformation twins blocked the motion of partial dislocations followed by increasing flow stress. The blocking of the partial dislocations by the twins could also be another reason that amplifies the serrations in the flow curves.

4. Conclusions

In conclusion, studies were done to understand the influence of preferentially segregating dopants on grain boundary relaxation, and the subsequent effect on plastic deformation mechanisms in nanocrystalline aluminum. The thermodynamic modeling revealed that magnesium dopants reduce the Gibbs free energy of mixing in the grain boundary region which stabilizes the nanostructure. The atomistic simulations showed that the preferential partitioning of magnesium dopants to the grain boundaries reduces the excess volume within this region which stabilizes the nanostructures. At low contents, the magnesium dopants were observed to initially partition to the grain boundaries, but once saturation of the grain boundaries was reached, excess dopants were accommodated in the crystalline interiors. Furthermore, it was found that the addition of the magnesium dopants even in the dilute limit, enhanced the strength of the nanocrystalline aluminum. Thus, increasing the dopant content will not necessarily result in increased stability and strength. The formation of large, disordered GBs in doped nanocrystalline aluminum under tensile load allowed it to accommodate the deformation and prohibit crack growth.

Acknowledgements

The authors gratefully acknowledge the financial support from US Department of Energy, Innovative Manufacturing Initiative (DEEE0009116), through the Advanced Manufacturing Office.

References

[1] Ovid'ko, I., A *et al, Prog. Mater Sci.* 94, 462–540 (2018).

[2] K.S. Kumar, H. Van Swygenhoven, S. Suresh, Acta Mater. 51 (2003) 5743-5774.

[3] H.A. Padilla, B.L. Boyce, Exp. Mech. 50 (2010) 5-23.

[4] D.H. Jeong, F. Gonzalez, G. Palumbo, K.T. Aust, U. Erb, Scr. Mater. 44 (2001) 493-499.

[5] Tellkamp, V. L. *et al.* Mechanical behavior and microstructure of a thermally stable bulk nanostructured Al alloy. *Metall and Mat Trans A* **32**, 2335–2343 (2001).

[6] Chen, Z., Analysis of controlled-mechanism of grain growth in undercooled Fe–Cu alloy. *J. Alloy. Compound.* **509**, 7109–7115 (2011).

[7] B. Han, "Improvement of toughness and ductility of cryomilled Al-Mg alloy via microstructural modification," *Met. Mat Trans A*, pp. 2081–2091, 2005.

[8] Koch, Carl C. "Structural nanocrystalline materials: an overview." *Journal of Materials Science* 42.5 (2007): 1403-1414.

[9] Suryanarayana, C., and C. C. Koch. "Nanocrystalline materials–Current research and future directions." *Hyperfine interactions* 130.1 (2000): 5-44.

[10] Suryanarayana, C. "The structure and properties of nanocrystalline materials: issues and concerns." *Jom* 54.9 (2002): 24-27.

[11] I. Ovid'ko, "Review on superior strength and enhanced ductility of metallic nanomaterials," *Prog Mater Sci*, pp. 462–540, 2018.

[12] Erwin, Steven C., et al. "Doping semiconductor nanocrystals." *Nature* 436.7047 (2005): 91-94.

[13] Xiao, Chenghe, et al. "Tensile behavior and fracture in nickel and carbon doped nanocrystalline nickel." *Materials Science and Engineering: A* 301.1 (2001): 35-43.

[14] Vo, N. Q., et al. "Reaching theoretical strengths in nanocrystalline Cu by grain boundary doping." *Scripta Materialia* 65.8 (2011): 660-663.

[15] Thangadurai, P., A. Chandra Bose, and S. Ramasamy. "Phase stabilization and structural studies of nanocrystalline La 2 O 3-ZrO 2." *Journal of materials science* 40.15 (2005): 3963-3968.

[16] Millett, Paul C., R. Panneer Selvam, and Ashok Saxena. "Molecular dynamics simulations of grain size stabilization in nanocrystalline materials by addition of dopants." *Acta materialia* 54.2 (2006): 297-303.

[17] J. Trelewicz and C. Schuh, "The Hall-Petch Breakdown in Nanocrystalline Metals: A crossover to glass-like deformation," *Acta Mater.*, 2007.

[18] N. Hansen, "Hall-petch relation and boundary strengthening," *Scr. Mater.*, 2004.

[19] H. Murdoch and C. Schuh, "Stability of Binary Nanocrystalline Alloys Against Grain Growth and Phase Separation," *Acta Mater.*, 2013.

[20] J. Trelewicz and C. Schuh, "Grain Boundary Segregation and Thermodynamically Stable Binary Nanocrystalline Alloys," *MIT Phys. Rev. B*, 2009.

[21] M. Saber, H. Kotan, and C.C. Koch, "Thermodynamic stabilization of nanocrystalline binary alloys," *J. Appl. Phys.*, 2013.

[22] T. Chookajorn, H. Murdoch, and C. Schuh, "Design of Stable Nanocrystalline Alloys," *Science*, 2012.

[23] H. Murdoch and C. Schuh, “Stability of Binary Nanocrystalline Alloys Against Grain Growth and Phase Separation,” *Acta Mater.*, 2013.

[24] M. Saber, H. Kotan, and C.C. Koch, “A predictive model for thermodynamic stability of grain size in nanocrystalline ternary alloys,” *J. Appl. Phys.*, 2013.

[25] Löffler J, Weissmüller J. Grain-boundary atomic structure in nanocrystalline palladium from x-ray atomic distribution functions. Phys Rev B Condens Matter. 1995 Sep 1;52(10):7076-7093. doi: 10.1103/physrevb.52.7076. PMID: 9979648.

[26] Byeong-Hyeon Lee, Sung-Hoon Kim, Jun-Hyoung Park, Hyung-Wook Kim, Jae-Chul Lee, “Role of Mg in simultaneously improving the strength and ductility of Al–Mg alloys,” Materials Science and Engineering: A, Volume 657, 2016, Pages 115-122.

[27] H. Murdoch and C. Schuh, “Estimation of Grain Boundary Segregation Enthalpy and its role in stable nanocrystalline alloy design,” *J. Mater. Res.*, 2013.

[28] A. R. Miedema, R. Boom, and F. R. De Boer, “On the Heat of Formation of Solid Alloys,” *J. Common Met.*, vol. 41, no. 2, pp. 283–298, 1975.

[29] H. Pierre. "Atomsk: A tool for manipulating and converting atomic data files." *Computer Physics Communications* 197 (2015): 212-219.

[30] H. Murdoch and C. Schuh, “Estimation of Grain Boundary Segregation Enthalpy and its role in stable nanocrystalline alloy design,” *J. Mater. Res.*, 2013.

[31] Y. Gutkin, *Woodhead Publishing Series in Metals and Surface Engineering* (2011) 329-374

[32] J. Hohl, P. Kumar, M. Misra, L.T Mushongera, Thermodynamic Stabilization of Nanocrystalline Aluminum, J Mater Sci 56, 14611–14623 (2021). https://doi.org/10.1007/s10853-021-06224-2

[33] Mendelev, M. I., et al. "Development of interatomic potentials appropriate for simulation of solid–liquid interface properties in Al–Mg alloys." *Philosophical Magazine* 89.34-36 (2009): 3269-3285.

[34] Stukowski, Alexander. "Visualization and analysis of atomistic simulation data with OVITO–the Open Visualization Tool." *Modelling and Simulation in Materials Science and Engineering* 18.1 (2009): 015012.

[35] A. Stukowski, *Model. Simul. Mat. Sci. Eng.* 20(4) (2012) 045021.

[36] J. Westbrook and D. Wood, “Embrittlement of grain boundaries by equilibrium segregation,” *Nature*, 1961.

[37] Weissmüller, J. "Alloy effects in nanostructures." *Nanostructured Materials* 3.1-6 (1993): 261-272.

[38] Haque, Md Amanul, and MT A. Saif. "Mechanical behavior of 30–50 nm thick aluminum films under uniaxial tension." Scripta Materialia 47.12 (2002): 863-867.

[39] Pun, Simon C., et al. "Nanocrystalline Al-Mg with extreme strength due to grain boundary doping." *Materials Science and Engineering: A* 696 (2017): 400-406.

[40] Kazemi, Amirreza, and Shengfeng Yang. "Atomistic study of the effect of magnesium dopants on the strength of nanocrystalline aluminum." *JOM* 71.4 (2019): 1209-1214.

[41] Lee, Byeong-Hyeon, et al. "Role of Mg in simultaneously improving the strength and ductility of Al–Mg alloys." *Materials Science and Engineering: A* 657 (2016): 115-122.

[42] Liu, X-Y., and James B. Adams. "Grain-boundary segregation in Al–10% Mg alloys at hot working temperatures." *Acta Materialia* 46 (10) (1998): 3467-3476.

[43] Xiao-Lei Wu, " Deformation twinning mechanisms in nanocrystalline Ni." Appl. Phys. Lett. 88, 061905 (2006).

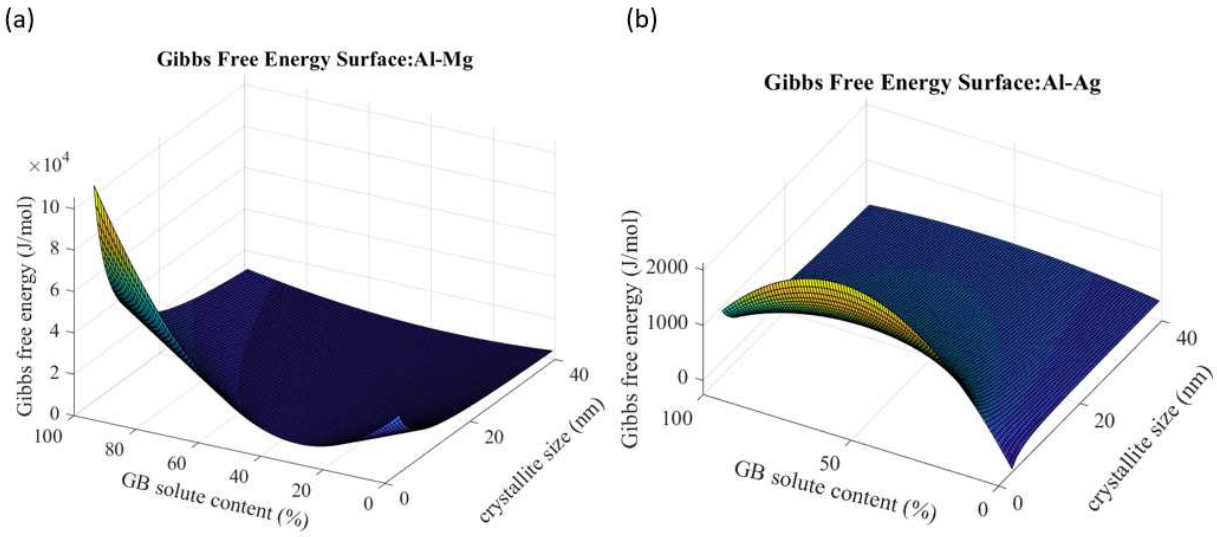

Figure 1: Gibbs free energy surface (a) NC Al-Mg example of stable nanocrystalline state (b) NC Al-Ag example of unstable nanocrystalline state.

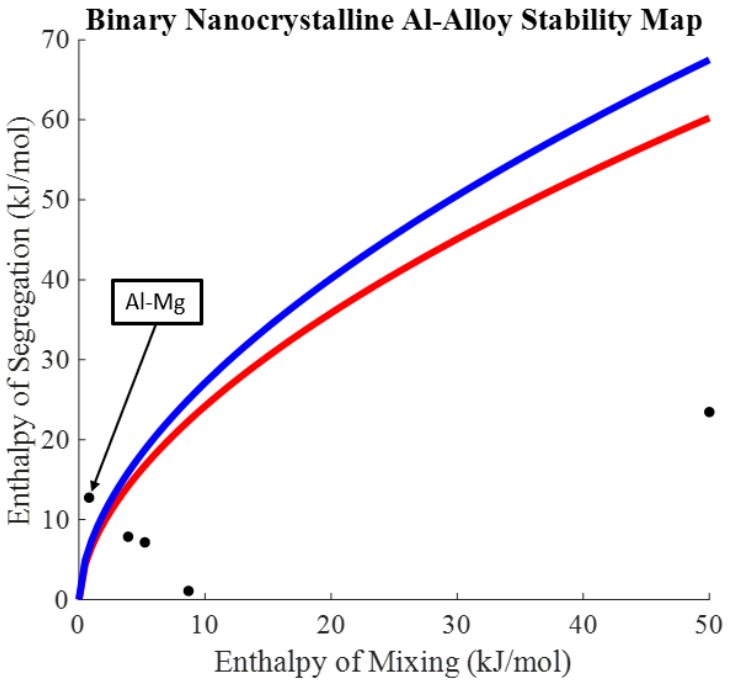

Figure 2: Nanocrystalline Aluminum empirical stability map generated from results of thermodynamic framework.

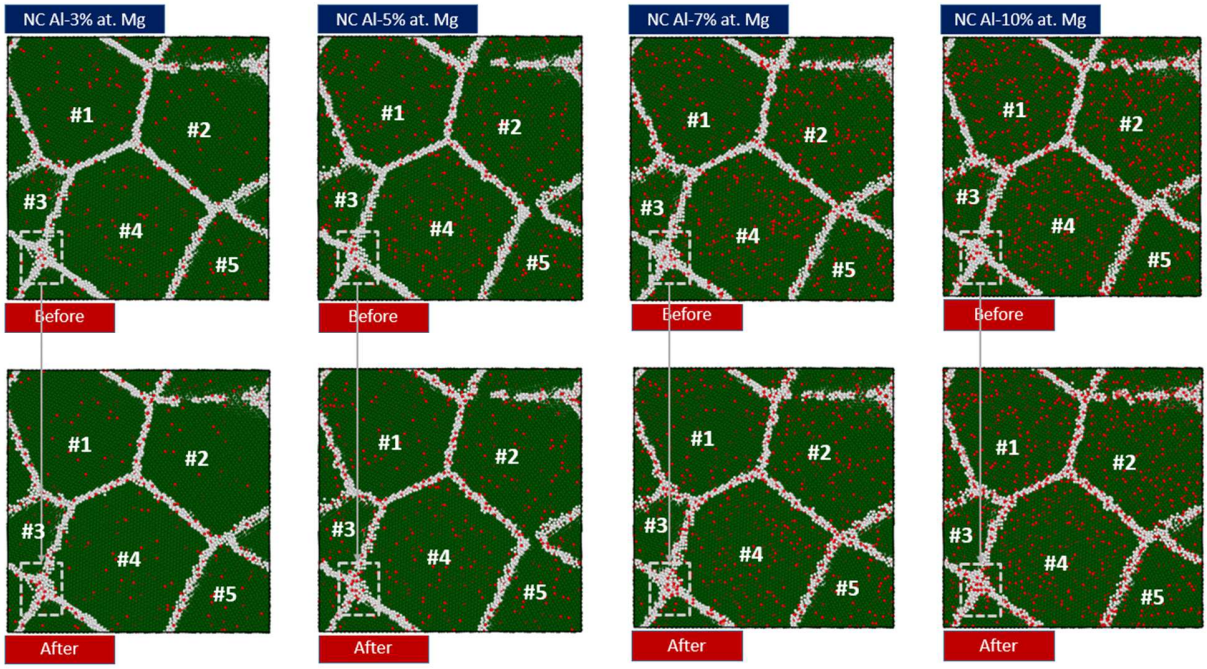

Figure 3: (a), (b), (c) and (d) 2D atomistic GB structures of NC-Al with 3, 5, 7 and 10 at. % Mg before and after dopant segregation, respectively. The square marked in the structures presents the change of dopant atoms in this GB region.

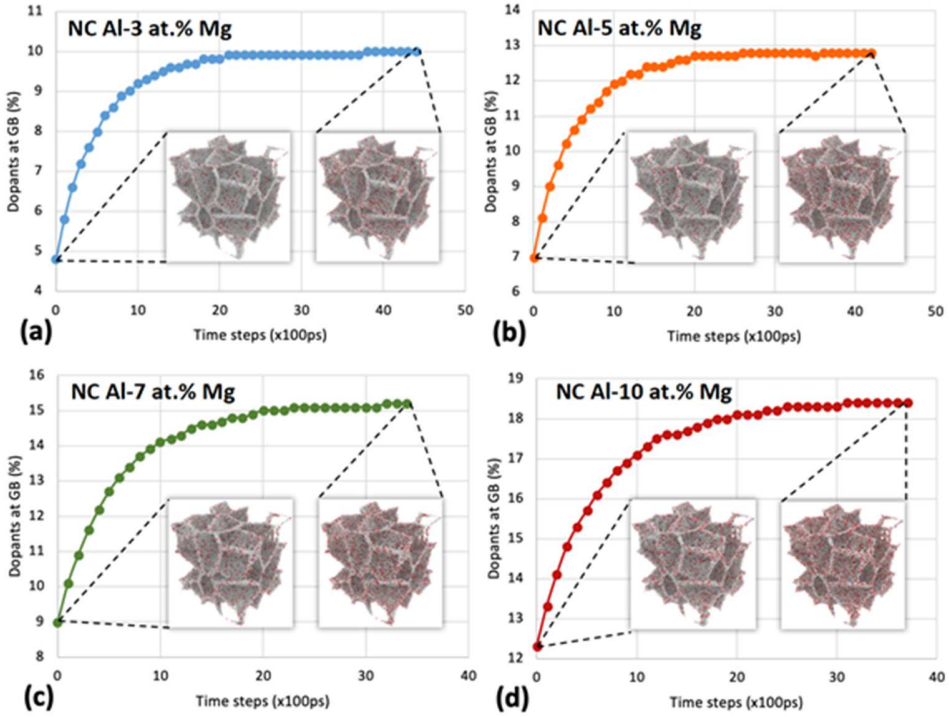

Figure 4: (a), (b), (c) and (d) The change of dopants during segregating at GB of NC-Al with 3, 5, 7 and 10 at. % Mg.

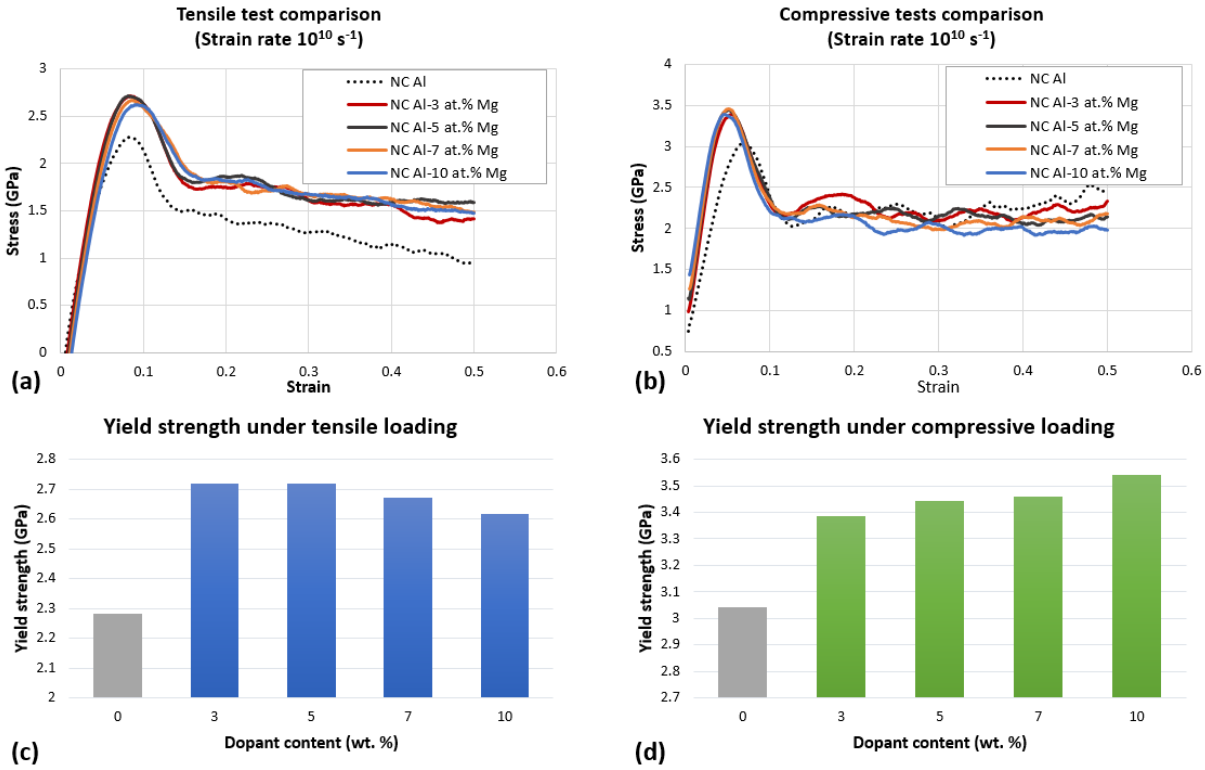

Figure 5: (a) and (b) strain stress behavior of pure NC Al and NC Al with 3, 5, 7 and 10 at. % Mg dopant contents under tensile and compressive load, respectively. Comparison of yield strength for pure NC Al and NC Al with dopant under (c) tensile and (d) compressive loading.

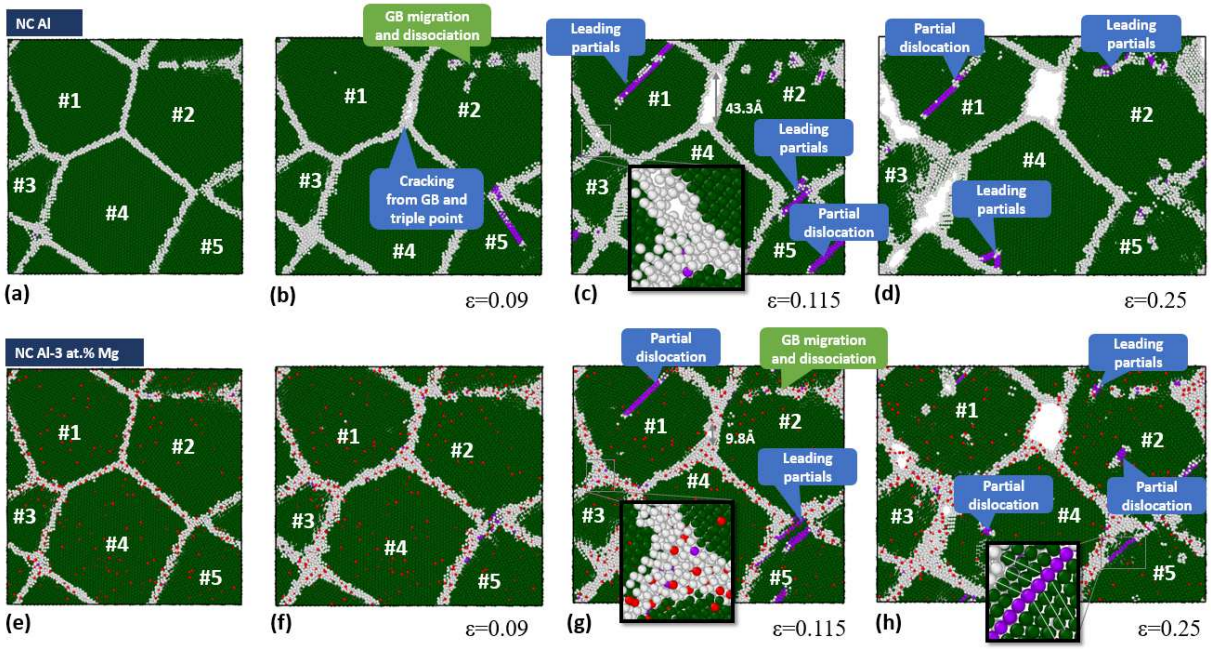

Figure 6: Comparison of the deformation of undoped and doped atomistic structures under a

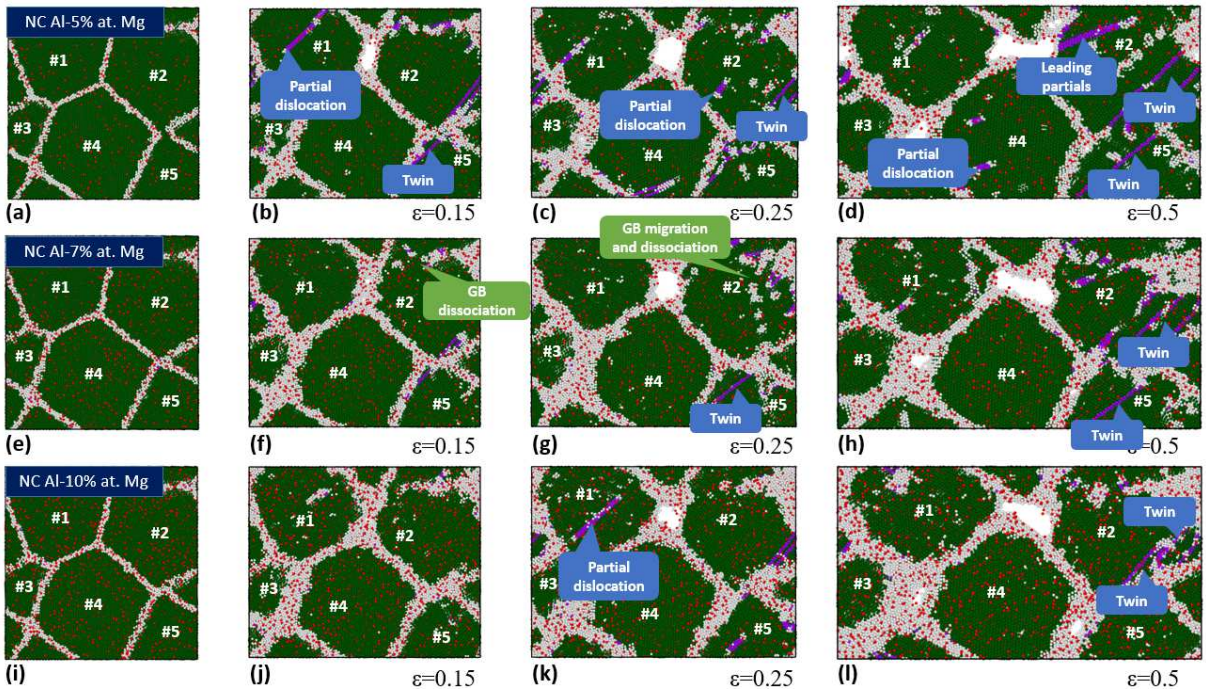

Figure 7: Comparison of atomistic structure for NC Al-5, 7 and 10 at. % Mg under a tensile load.

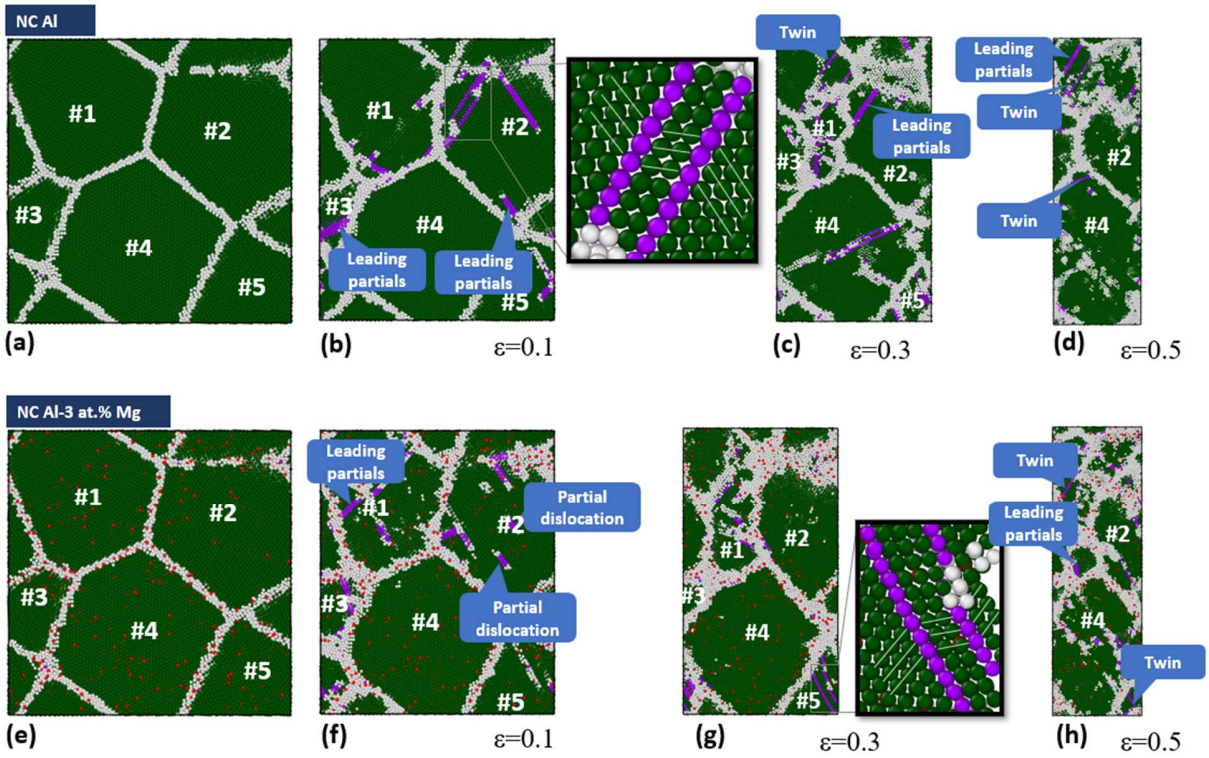

Figure 8: Comparison of atomistic structure for NC Al and NC Al-3 at. % Mg under a compressive load.